Particle Clustering and Jetting in a Cylindrical Shock Tube

Tao Xu[1], Fue-Sang Lien[2], and Fan Zhang[2,3]

[1]Waterloo CFD Engineering Consulting Inc., Waterloo, ON, Canada

[2]University of Waterloo, Waterloo, ON, Canada

[3]Defence R&D Canada – Suffield, Medicine Hat, AB, Canada

1 Introduction

It is widely observed in volcanic eruptions, supernovae and heterogeneous explosive detonation that expansion of condensed-phase particles forms clusters and coherent jets. Detonation of an explosive mixture containing densely-packed bulk liquid or solid particles provides a good approach in studying these dense particle flows inherently with particle clustering and jetting, which are generated at the very early stage of the particle dispersal process, persisting then for a long time [1-2]. Despite progress to date in both experimental and numerical studies, the true mechanisms causing particle clustering and jetting are still unknown due to the complex phenomena involved in the early phase of expansion, including shock-particle interaction, particle collision and turbulence.

In the present paper, a cylindrical shock tube using a packed annular particle bed (also referred to as a "powder bed" herein) placed in the driven section with its far end adjacent to open air is numerically investigated, in order to understand the fundamental phenomena and physical mechanisms associated with the particle clustering and jet structures in the shock-compacting and expanding dense solid flow. Numerical simulations at mesoscale are performed over a range of parameters, including driver gas, particle morphology and distribution, and powder bed configuration.

2 Meso-scale Numerical Methodology

A HLLC3D-IBM code is developed for the present study to resolve explicitly particle collision and agglomeration, particle-shock, particle-wake/boundary-layer and particle-turbulence interactions [3]. The governing equation is the standard two-dimensional Navier-Stokes equation including the viscous stress tensor and the heat flux. The HLLC approximate Riemann solver combined with the MUSCL-Hancock method are used to evaluate the advective fluxes. A simple log-law-based near-wall treatment in conjunction with a monotone integrated large-eddy simulation model MILES [4] is used. Ghost-cell immersed boundary method (GCIBM) proposed by Tseng & Ferziger [5] is implemented, in which the "no-slip" condition on a solid surface is used to infer the boundary conditions required for the ghost cells.

Particle velocities at pre- and post-collision instants for two-particle collision are given by [6]

$$\mathbf{u}'_{p,1} = \mathbf{u}_{p,1} - \frac{m^{eff}}{m_{p,1}}(1+\varepsilon)(\mathbf{u}_{p,12}\cdot\mathbf{e})\mathbf{e}$$
$$\mathbf{u}'_{p,2} = \mathbf{u}_{p,2} + \frac{m^{eff}}{m_{p,2}}(1+\varepsilon)(\mathbf{u}_{p,12}\cdot\mathbf{e})\mathbf{e} \tag{1}$$

where ε is the coefficient of restitution, For $\varepsilon = 1$, total kinetic energy is conserved, and the collision occurs elastically. For $\varepsilon = 0$, the complete energy associated with the relative motion is lost or dissipated, and the particles are bound together after a collision, which is classified as an inelastic collision. The effective mass is $m^{eff} = \frac{m_{p,1}m_{p,2}}{m_{p,1}+m_{p,2}}$. An extension of Eq. (1) to multiple-particle collisions is developed and the detailed description can be found in [3].

The computational domain of the present cylindrical shock tube problem is depicted in Fig. 1 (at t = 0) for a baseline test case (or referred to as the "Basic" case in Table 1), which consists of a circular high pressure gas driver section and an annular driven section, consisting of a solid powder bed filled with air in void regions adjacent to the driver section. In the far field of the driven section, the standard temperature and pressure (STP) condition for air is assumed: 1 atm and 25 °C. The air is assumed to follow the ideal gas law. This "Basic" test case contains 300 particles in 7 ring-shaped layers with a solid volume fraction of 0.6 in the powder. From the inner to the outer surface of the powder bed, the particle number of each layer are 25, 31, 40, 43, 48, 54 and 59 and the corresponding layer radius from the center of the driver section are 0.684, 0.832, 0.980, 1.128, 1.270, 1.414 and 1.560. The size of the computational domain is 9.6×9.6 (in dimensionless unit) covered with 1000×1000 structured grid cells for all test cases in this paper. The Neumann boundary conditions are applied to all far-field boundaries. The typical grid resolution to cover a particle is about 25×25 which has been chosen after a grid convergence study. The initial conditions and results presented in this paper are dimensionless with reference quantities D_c, ρ_r and a_r, where D_c is the diameter of the circular driver section, ρ_r and a_r are the air density and speed of sound in the STP condition, respectively.

3 Mechanism for the Formation of Particle Jet Structures

The parameters corresponding to the "Basic" test case are listed in the first row of Table 1. Figure 1 shows the simulated particle dispersal process for the "Basic" test case at four different (dimensionless) times: t = 0, 0.74, 1.11 and 1.51. At the beginning, the high pressure driver gas is squeezed into the powder bed, and forms several micro jets between the solid particles in the first layers. The resulting shock fronts are propagating radially in voids between particles (at t = 0.74). At the same time, the high pressure gas drives particles to form a chain of particles (see, e.g., t = 1.11 and 1.51) through collision. This results in motion of particles in the outermost layer of the powder bed ahead of shocks. The shocked flow driven by the gas jets emanating from voids between particles, and chaining of solid particles generated by collision fracture the powder bed, thus forming clusters of particles (or particle jets) as shown at t = 1.11. The total number of particle jets remains the same in the present case at a later time of t = 1.51.

As shown in Fig. 1, the driver gas centered at the location of (x,y) = (4.8,4.8) in Zone A is released after t = 0. The interface between the driver section and the powder bed is disturbed and becomes unstable due to the passage of the shock. The spike-like gas structures at the interface emerge in void regions between particles in the innermost layer of the powder bed, and develop into incipient micro gas jets. As the shock fronts propagate through the powder bed, the expanding gas jets and shocked flow ahead separate the particles, while the inelastic collision results in agglomeration of particles. The close particle-to-particle interactions cause the outermost layer of the powder bed to move ahead of the shock fronts as seen at t = 0.74. It is clear from the subfigure at t = 0.74 that the incipient particle jets have already formed. Based on this observation, the exact time corresponding to the formation of particle jet structures can be defined as the time when the outer surface of the powder bed is being perturbed. The spikes [i.e., the heavy (or high-density) fluid penetrates into the light (or low-density) fluid] or bubbles (i.e., the light fluid penetrates into the heavy fluid) disturbed by shocks lead to large shears between particles and their surrounding fluid, thus providing additional lateral forces acting on the particles. At t = 1.11, the voids between clusters of particles (or particle jets) due to inelastic collision can be clearly seen. The inter-particle forces at this time cancel each other within the (agglomerated) particle jets. At time t = 1.51 and after (now shown), the jet structure is maintained and, each particle jet (typically containing 7-15 particles) moves outwards (or radially) in time.

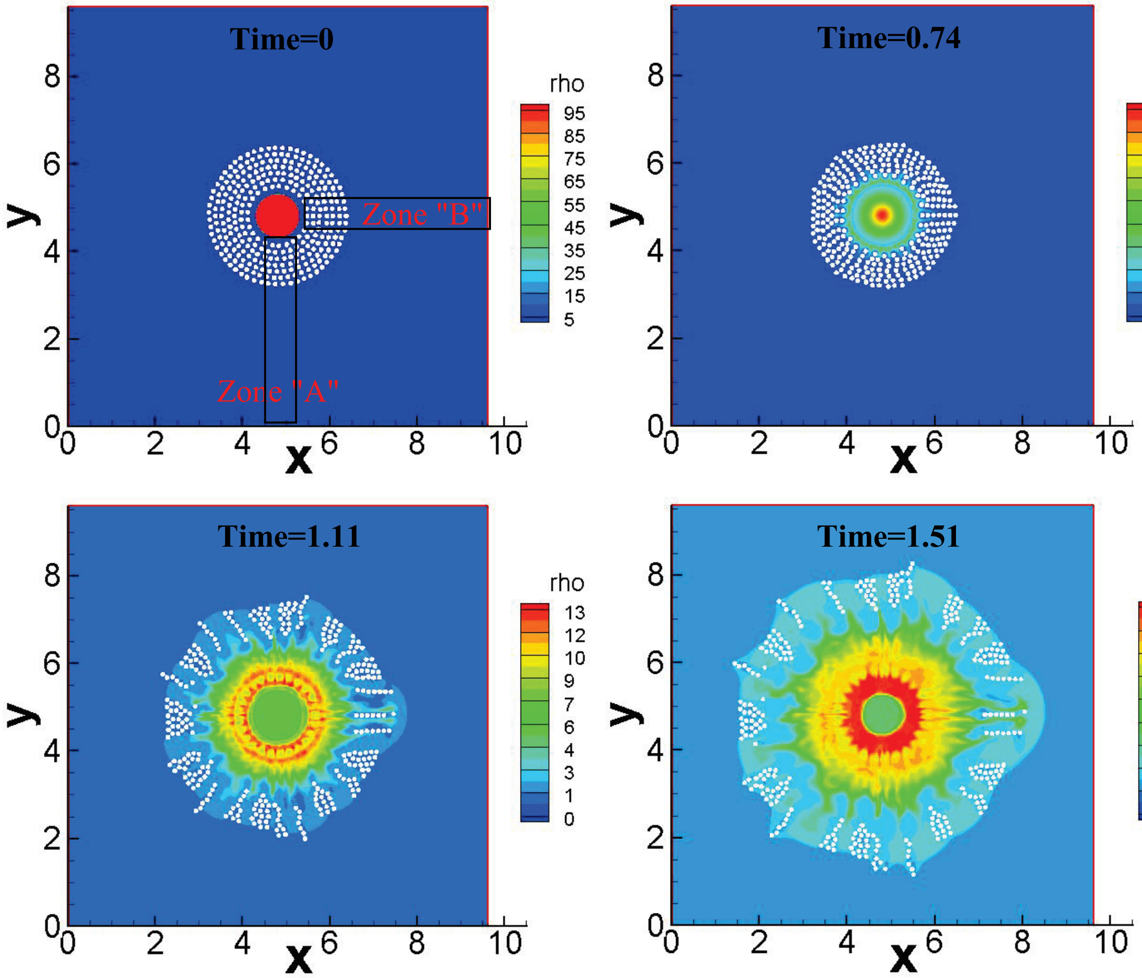

Fig. 1: Density contours of particle dispersal at four different times for the "Basic" test case.

The spike-like gas structures between the moving particles are initially induced by the passage of shocks, which develop later into the incipient micro gas jets. Most of the research about Richtmyer-Meshkov (RM) instability were focused on single-phase flows, and analysis of multiphase RM instability is still in its infancy. The Rayleigh-Taylor (RT) instability between the high density gas in the driver section and its surrounding low density air is not likely the underlying mechanism for the formation of particle jets, because the time scale corresponding to the fracturing of the powder bed demonstrated here is much smaller than that for the growth of RT instability. Furthermore, the present mesoscale results show that the maximum velocity of the gas jets is about 1.9, while the maximum velocity of particles in Zone A is about 1.0 at t = 0.38. This suggests that large velocity differences (or shears) exist between particles and their surrounding fluid. In general, the mesoscale results suggest that the initial perturbations at the interface between the driver and the driven sections are triggered by the shock, and then further enhanced by the presence of the densely-packed moving particles, which result in the formation of micro gas jets within voids in the innermost layer of the powder bed.

Subsequently from here, the outward motion of innermost layer particles, initially driven by the high pressure driver gas, results in sequential inelastic collisions to chain particles radially while the shears due to particle/gas-jet interactions cause the motion and inelastic collision (or clustering) of particles laterally. Both the gas jets with shocked flows ahead and the inelastic collision of particles, therefore fracture the powder bed radially, while the shears due to particle/gas-jet interactions cause the motion and inelastic collision (or clustering) of particles laterally. Overall, we believe that the most probably underlying causes for the formation of particle jet structures are the driver gas jet flow induced by the shock wave as it passes through the initial gaps between the particles in the innermost layer of the powder bed, and the chaining of solid particles by inelastic collision. The shear flow between particles and surrounding fluid further accelerates the particle jet formation and growth.

Since the movement of the outer surface of the powder bed can be easily detected, the corresponding time can be chosen to determine the jet forming time. Physically, the motion of the outer surface of the powder bed is caused by particle-to-particle collision and fluid movement within the voids between particles. The jet forming time based on the initial motion of the outer surface of the powder bed can therefore be estimated as $t_{jet} = \frac{1}{2}\frac{D_p - D_c}{U}$, where U is an average radial speed of void fluid and particles, D_p is the diameter of the outer surface of the powder bed and D_c is the diameter of the central circular charge; i.e., the high-pressure driver section in the present work. Alternatively, one can use the expansion velocity of the solid particle layer, which is very close to the so called Gurney velocity as a function of total energy of the charge (explosive or a driver section) and the mass ratio of powder bed to charge. If simply assuming U to be the shocked fluid velocity, the corresponding jet forming time is determined to be at around t = 0.6 for the "Basic" test case.

4 Parameters Affecting the Number of Particle Jets

To explore the dependence of the number of particle jets on various parameters, mesoscale simulations have been carried out for a variety of cases listed in Table 1. From the mesoscale simulations, the total number of particle jets for each test case is counted when they are fully developed and are listed in the third last column of Table 1. The patterns of the particle jets are maintained after the formation of jet structures is completed in early times. As shown in the first four rows of Table 1, the number of particle jets decreases as the inertia of powder bed increases (i.e., an increase in either total particle number or material density of particle) at a given driver pressure. The effect of particle size on the number of particle jets is not apparent within the size range studied (only two sizes are investigated here). Furthermore, as shown in the first, sixth and seventh rows of Table 1, namely, the "Basic", "Pressure2" and "Pressure3" cases, the number of particle jets increases as the driver pressure increases, which serves as the main driving force for particle dispersal.

The number of particle jets also depends on how particles are packed in the powder bed, as indicated in the "Random" test case listed in row 8 of Table 1. In comparison with the "Basic" test case, the number of particle jets is reduced from 23 to 21, indicating that higher resistance exists for the randomly-packed case compared to the uniformly-packed case. The number of particle jets remains unchanged when the restitution coefficient is increased from 0 (fully inelastic) to 0.5 (partial inelastic). A value of restitution coefficient chosen to be between 0 and 0.5 appears realistic in the high explosive dispersal of particles, where the shock pressure can reach several gigapascals in the early compaction phase of detonation, so that most of the particle collisions can be considered as inelastic collision. More simulations may still be needed for the restitution coefficient to be above 0.5, which are numerically challenging due to very small time steps required to ensure stability.

In order to further confirm that the maximum number of particle jets must be consistent with the number of particles in the innermost layer of the powder bed, a new test case entitled "Inner Layer" shown in the last row of Table 1 is created with a powder bed configuration different from the those listed in Table 1. The number of fully developed particle jets is 17 for the "Inner Layer" case and 25 for the "Layer3" case. This further confirms that the maximum number of particle jets is solely determined by the number of particles in the innermost layer of the powder bed.

Following the above parametric studies to investigate the mechanisms for the formation of particle jets, an empirical formula to estimate the number of particle jets is proposed: $N_{jet} = \mathrm{int}(\alpha \frac{\pi D_c}{d_s + \beta})$, where D_c, d_s and β are the diameter of the driver section, mean particle diameter and the average gap between particles (0.025 in this work), respectively. Assuming inelastic collision and without considering the influence of random particle distributions for simplicity, α can be assumed to be $\alpha = 1 - m\left(M^*/P^* + b\right)^n$, where M^*, P^* are the dimensionless mass of total particles and pressure ratio of driver gas to air, respectively. N_{jet} above can then be rewritten in the following form:

$$N_{jet} = \mathrm{int}\left[\left(1 - 0.075(\frac{M^*}{P^*} + 0.7)^{1.02}\right)\frac{\pi D_c}{d_s + \beta}\right] \qquad (2)$$

where the coefficients are obtained by curve fitting based on the mesoscale results. The estimated numbers of particle jets from Eq. (2) are listed in the second last column of Table 1. For most cases listed in Table 1, a good agreement between the number of particle jets counted from the mesoscale solutions and that estimated with Eq. (2) is achieved.

Table 1: The test matrix and conditions.

Test case title	Total particles in domain	Gas p and ρ ratio	Particle radius	Restitut. coef. ε	Random-ness	Particle density	Number of particle jets	Number of particle jets from Eq. (34)	Particle volume fraction
Basic	300	100:1	0.05	0	No	10	23	23	0.6
Layer3*	96	100:1	0.05	0	No	10	25	24	0.6
Layer5#	187	100:1	0.05	0	No	10	24	23	0.6
Particle Density	300	100:1	0.05	0	No	10 & 50	22	23	0.6
Particle Size	300	100:1	0.05 & 0.03	0	No	10	23	22	0.6
Pressure2	300	10:1	0.05	0	No	10	18	18	0.6
Pressure3	300	1000:1	0.05	0	No	10	25	24	0.6
Random	300	100:1	0.05	0	Yes	10	21	-	0.6
Restitution	300	100:1	0.05	0.5	No	10	23	-	0.6
Inner Layer@	183	100:1	0.1	0	No	10	17	15	0.28

*: the first 3 particle layers are included in the domain; #: the first 5 particle layers are included in the domain; @: 6 particle layers and 17 particles in the innermost layer of powder bed, while all other cases have 25 particles in the innermost layer. The radius of the driver section is 0.5 for all cases except the "Inner layer" case, where the corresponding radius is 0.8 to accommodate larger particles.

5 Conclusions

The present work is stimulated by the interest in understanding the physical mechanisms associated with the particle clustering and coherent jet formation observed in real world including volcanic eruptions, supernovae and heterogeneous explosive detonation. Clustering and coherent jetting of particles are fundamental phenomena in supersonic dense particle flows. To gain a better understanding of jetting of particles, mesoscale simulations are conducted about a cylindrical shock tube problem, in which a central high pressure/high density driver section surrounded by a densely packed powder bed in air in the driven section. The immersed boundary method (IBM) and a novel multi-particle inelastic collision model are incorporated into the two-dimensional Navier-Stokes equations. Parameters studied include the driver gas pressure, particle distribution, particle morphology, and packed powder bed configuration.

The simulation results indicate that as the shock passes through the interface between the driver section and powder bed, micro gas jets are formed in voids between particles in the innermost layer of the powder bed. While the gas jets penetrate the powder bed in the radial direction and propel the particles laterally, the driver gas pushes outward motion of innermost layer particles, resulting in sequential inelastic collisions to chain particles radially. The micro gas jets also incur a large shear due to velocity differences between particles and their surrounding fluid, which further propels particles laterally. Thus, the driver gas jets and the chaining of solid particles by inelastic collision are the most probably underlying causes for the formation of particle jet structures. Since the number of the micro gas jets is the same as the number of particles in the innermost layer of powder bed, the latter provides a maximum or upper bound of the number of particle jets as demonstrated in the mesoscale simulations. As the mass of powder bed (related to the total number of particles, number of particle layers and material density of particle) increases or the driver pressure decreases, some weak perturbations at the interface between the driver section and the powder bed, caused by the passage of the shocks, may not develop into sustainable micro gas jets to fracture the powder bed. This results in fewer number of particle jets than the number of particles in the innermost layer of powder bed. Thus, the number of particle jets is mainly a function of the number of particles in the innermost layer of powder bed adjacent to the driver section, and the mass ratio of powder bed to gas in the driver section or the ratio of the dimensionless powder bed mass to the pressure ratio of driver to air. The random distribution of particles could further reduce the number of particle jets formed due to high local resistance.

The real-world-scale dispersal of a packed condensed-phase particle bed is much more complicated and involve more complex mechanisms responsible for particle clustering and jetting. The diverging shock tube flow containing dense particles provides a good starting point to study the fundamental aspects of a supersonic dense particle flow, which remains an open area. Extension of the present work to (re-)examine factors such as more particles in powder bed, higher pressure and density ratios corresponding to high explosive, particle deformation, compaction effects that occur at these pressures, particle casing effects, combustion and finer meshes will require further investigations.

References

[1] Frost, D.L., Gregoire, Y., Goroshin, S., Zhang, F. (2011). Interfacial instabilities in explosive gas-particle flows. In: Proc. 23rd ICDERS, Irvine.

[2] Ripley, R.C., Donahue, L., Zhang, F. (2011). Jetting instabilities of particles from explosive dispersal. Shock Compression of Condensed Matter – 2011, pp. 1615-1618.

[3] Xu, T., Lien, F.-S., Ji. H., Zhang, F. (2013). Formation of particle jetting in a cylindrical shock tube. Shock Waves (in revision).

[4] Boris, J., Grinstein, F., Oran, E., Kolbe, R. (1992). New insights into large eddy simulation. Fluid Dynamics Research 10: 199.

[5] Tseng, Y.H., Ferziger, J.H. (2003). A ghost-cell immersed boundary method for flow in complex geometry. J. Comput. Phys. 192: 593.

[6] Brilliantov, N.V., Poschel, T. (2004). Kinetic theory of granular gases. Oxford University Press.